Tuning of the Rheological Properties and Thermal Behavior of Boron-Containing Polysiloxanes

Rodrigue Ngoumeni-Yappi,[†] Claudia Fasel,[†] Ralf Riedel,*[,†] Vladislav Ischenko,[‡] Eckhard Pippel,[‡] Jörg Woltersdorf,[‡] and Jürgen Clade[§]

Institut für Materialwissenschaft, Technische Universität Darmstadt, Petersenstrasse 23, D-64287 Darmstadt, Germany, Max-Planck-Insitut für Mikrostrukturphysik, Weinberg 2, D-06120 Halle, Germany, and Fraunhofer-Institut für Silicatforschung, Neunerplatz 2, 97082 Würzburg, Germany

Received November 2, 2007. Revised Manuscript Received February 18, 2008

The rheological behavior of boron-containing poly(organosiloxanes) and their thermal decomposition were studied in order to evaluate the spinnability of these preceramic polymers, which might be suitable for the production of high-temperature-resistant ceramic fibers in the SiBCO system. The polymers were synthesized by methanolysis of tris(1-(dichloro(methyl)silyl)ethyl)borane and subsequent hydrolysis of the reaction product. Three different polymers were obtained by varying the amount of water during the hydrolysis step. The degree of cross-linking and hence the viscosity of the resulting polymer increased with the amount of water as analyzed by rheological measurements. The spinnability of polymers is affected by their flow characteristics, especially by their visco-elasticity, expressed by the dynamic moduli G' (storage modulus, indicating elastic properties) and G'' (loss modulus, indicating viscous properties), respectively. The thermal behavior of the three samples was analyzed in situ during the pyrolysis process between room temperature and 1400 °C, and ex situ by HREM and EELS after thermal decomposition of the samples. The ceramic yield was determined to be 45 wt % for the polymer with the lowest cross-linking degree and increased up to 75 wt % in case of the highly cross-linked polymer.

1. Introduction

Melt spinning is a widely used process for manufacturing of commercial fibers for different high-temperature applications, such as reinforcing materials in ceramic matrix composites (CMCs). The dependence of the fiber properties on their chemical composition and on the processing sequence has been investigated in the last decades. Although oxide fibers show high oxidation resistance and chemical stability, their tensile strength and creep resistance have to be improved in particular at elevated temperatures.[1–3] Because silicon-carbide-based ceramic fibers have shown remarkable qualities as reinforcing materials in CMCs, the improvement of their thermal stability and chemical resistance was the main research focus in recent years.[4–11] Thus, silicon carbide fibers with low oxygen content have been developed for high-temperature applications and the production of low-cost nonoxide fibers with enhanced properties is still a great challenge.

It was shown that the microstructure of SiC and SiC(O) fibers obtained after pyrolysis of polycarbosilane (PCS) consisted of β-SiC, free carbon, and in the case of SiC(O) fibers, of an amorphous silicon oxycarbide phase.[12] The presence of carbon in amorphous SiCO significantly increases the viscosity by about 2 orders of magnitude if compared with that of vitreous silica.[13] At temperatures exceeding 1000 °C, a pronounced redistribution of bonds in the SiCO matrix resulting in the formation of SiC_4 and SiO_4 coordination units could be analyzed by ^{29}Si MAS NMR investigations. This microstructural evolution occurred at lower temperature for samples with lower carbon content and shifted to higher temperature for SiCO ceramics with enhanced C content. Accordingly, the crystallization temperature of β-SiC was found at about 1200 °C for SiCO with low C content, whereas for the carbon-rich materials, the annealing temperature increased up to 1400 °C to promote crystallization.[14] In another work, the remarkable resistance of silicon oxycarbide toward crystallization, phase separation is reported to occur above 1300 °C and the SiCO ceramics partition into silicon carbide and silica.[15] The crystallization is accompanied by a weight loss, resulting from the carboth-

* Corresponding author. E-mail: riedel@materials.tu-darmstadt.de.
[†] Technische Universität Darmstadt.
[‡] Max-Planck-Insitut für Mikrostrukturphysik.
[§] Fraunhofer-Institut für Silicatforschung.

(1) Levi, C. G.; Yang, J. Y.; Dalgleish, B. J.; Zok, F. W.; Evans, A. G. *J. Am. Ceram. Soc.* **1998**, *81* (8), 2077–2086.
(2) Kramb, V. A.; John, R. *J. Am. Ceram. Soc.* **1999**, *82* (11), 3087–3096.
(3) Heathcote, J. A.; Gong, X. Y.; Yang, J. Y.; Ramamurty, U.; Zok, F. W. *J. Am. Ceram. Soc.* **1999**, *82* (10), 2721–2730.
(4) Yajima, S.; Hayashi, J. *Chem. Lett.* **1975**, (9), 931–934.
(5) Taki, T.; Okamura, K. *J. Mater. Sci. Lett.* **1988**, *7* (3), 209–211.
(6) Baldus, P.; Jansen, M. *Science* **1999**, *285* (5428), 699–703.
(7) Cinibulk, M. K.; Parthasarathy, T. A. *J. Am. Ceram. Soc.* **2002**, *85* (11), 2703–2710.
(8) Rocabois, P.; Chatillon, C. *Surf. Coat. Technol.* **1993**, *61* (1−3), 86–92.
(9) Jaskowiak, M. H.; Dicarlo, J. A. *J. Am. Ceram. Soc.* **1989**, *72* (2), 192–197.
(10) Saha, A.; Shah, S. R. *J. Am. Ceram. Soc.* **2003**, *86* (8), 1443–1445.
(11) Yajima, S.; Hayashi, J. *Nature* **1976**, *261* (5562), 683–685.
(12) Shimoo, T.; Morisada, Y. *J. Am. Ceram. Soc.* **2000**, *83* (12), 3049–3056.
(13) Rouxel, T.; Soraru, G. D. *J. Am. Ceram. Soc.* **2001**, *84* (5), 1052–1058.
(14) Brequel, H.; Parmentier, J. *Chem. Mater.* **2004**, *16* (13), 2585–2598.

10.1021/cm703137e CCC: $40.75
Published on Web 05/08/2008

ermal reduction of silica in materials with high carbon content,[16] leading to a significant decrease of their mechanical properties.

The incorporation of boron in the silicon oxycarbide network was found to be appropriate in order to avoid the segregation of silica (cristobalite).[17,18] ^{11}B MAS NMR spectra clearly displayed the presence of B−O bonds, causing a reduction of [SiO_4] coordination units in the SiBCO network.[19,20] RAMAN spectroscopy measurements showed the decrease of free carbon and enhanced SiC formation with increasing boron content.[17,18,20] These findings indicate that ceramic fibers derived from boron-containing poly(organosiloxanes) are promising candidate materials for high-temperature applications.

The processing sequence of ceramic fibers starting from preceramic polymers involves four main steps: (i) polymer synthesis, (ii) fiber spinning, (iii) fiber curing, and (iv) pyrolysis of the cured fiber. It is worth mentioning that the second step, i.e., the fiber spinning, strongly depends on the polymer viscosity and thus is influenced by the synthesis route. The rheological behavior and spinnability of polymers are affected by their molecular structure because of the relationship between viscosity and molecular weight.[21,22] The effects of the polymer concentration on the rheology was studied in the case of chemically cross-linked vinyl alcohol near the gelation threshold.[23] It was found that the gelation time decreased with increasing amount of cross-linking agent. In addition, rheological studies conducted on several organic side chain dendritic polymers showed greater zero shear viscosity values for monomers with a bigger side group.[24]

Due to the well-known behavior of organic polymers, it is expected that the rheological properties and the spinnability of SiBCO preceramic polymers depend significantly on the degree of cross-linking of the monomer units. In the present work, we used tris(1-(dichloro(methyl)-silyl)ethyl)borane (**TDB**) as the monomer-containing six Si−Cl groups, which are all capable of contributing to cross-linking. A maximum degree of substitution for these Si−Cl groups can be reached by reaction of the monomer with stochiometric or excess methanol or water. If the resulting groups can polycondense at low temperatures (e.g., silanol groups, Si−OH), a highly cross-linked polymer with Si−O−Si bridging units having a high viscosity is obtained. If, however, the substituted functional groups cannot readily condense at low temperatures (e.g., alkoxysilane groups, Si−OR), the viscosity remains low enough to enable the polymer to cure at higher temperatures, e.g., promoted by water vapor via hydrolysis.

In the present work, we used methanol to stoichiometrically replace Si−Cl groups in the monomer **TDB** by Si−OCH_3 in a first step. In a second step, the Si−OCH_3 groups are hydrolyzed to condensable silanols, Si-OH. This combination of methanolysis and partial hydrolysis allows one (i) to adjust the degree of cross-linking of the resulting organosilicon polymer, and hence, (ii) to tune the rheological properties as well as the spinnability of the preceramic polymer.

2. Experimental Section

All reactions described below were carried out in argon using Schlenk techniques.[25] Dichloromethylvinylsilane and borane dimethylsulphide were obtained from Aldrich (Milwaukee, WI) and used without further purification.

2.1. Synthesis. The synthesis of the polymers was performed in three steps: (i) synthesis of tris(1-(dichloro(methyl)silyl)ethyl)borane monomer **TDB** (reaction 1), (ii) methanolysis of the monomer (reaction reaction 2) and (iii) partial hydrolysis and polycondensation of methanolyzed **TDB** (reaction 3).

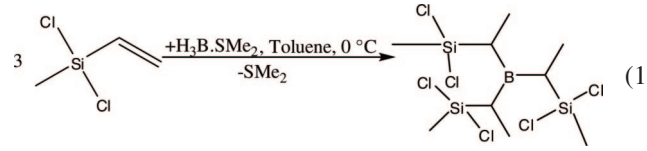

(1)

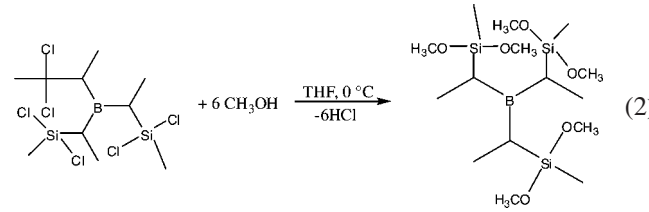

(2)

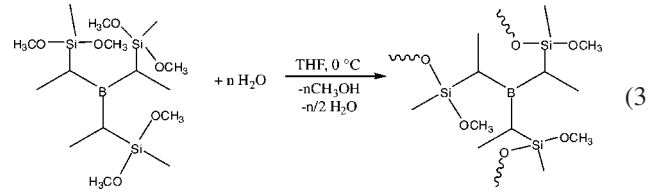

(3)

The boron-containing monomer was prepared as reported by Kienzle:[26] 100 mL (108.5 g, 0.76 mol) of commercially available dichloromethylvinylsilane was put in a 1 L Schlenk flask equipped with a magnetic stir bar, dissolved in toluene, and cooled to 0 °C. After the solution was stirred for 30 min, 23.6 mL (19 g, 0.25 mol) of borane dimethylsulphide was added dropwise and the solution was stirred at room temperature for 30 h to obtain 107 g (98%) of **TDB** after removing the solvent by distillation under reduced pressure at 40 °C (reaction 1). The isolated product was characterized by mass spectrometry and multi nuclear NMR: *m/z* 400.9 [(M − Cl)$^+$, 0.8]; 294.9 [(M − $CH(CH_3)SiCl_2CH_3$)$^+$, 100]; 153.0. [(M − $(CH(CH_3)SiCl_2CH_3)_2$)$^+$, 10]. ^{11}B-NMR spectroscopy of **TDB** shows one signal at 84.4 ppm, and two main signals at 28 and 33 ppm were observed in the ^{29}Si NMR spectrum that were due to the presence of stereoisomers.[26]

(15) Kleebe, H. J.; Turquat, C. *J. Am. Ceram. Soc.* **2001**, *84* (5), 1073–1080.
(16) Saha, A.; Raj, R. *J. Am. Ceram. Soc.* **2007**, *90* (2), 578–583.
(17) Liebau, V.; Hauser, R. *C. R. Acad. Sci., Ser. IIc: Chim.* **2004**, *7* (5), 463–469.
(18) Klonczynski, A.; Schneider, G. *Adv. Eng. Mater.* **2004**, *6* (1−2), 64–68.
(19) Wootton, A. M.; Lewis, M. H. *J. Sol−Gel Sci. Technol.* **1998**, *13* (1−3), 1001–1004.
(20) Soraru, G. D.; Babonneau, F. *J. Non-Cryst. Solids* **1998**, *224* (2), 173–183.
(21) Weijermars, R. *Appl. Phys. Lett.* **1986**, *48* (2), 109–111.
(22) Dvornic, P. R.; Jovanovic, J. D. *J. Appl. Polym. Sci.* **1993**, *49* (9), 1497–1507.
(23) Kjoniksen, A. L.; Nystrom, B. *Macromolecules* **1996**, *29* (15), 5215–5222.
(24) Jahromi, S. J.; Palmen, H. M. *Macromolecules* **2000**, *33* (2), 577–581.
(25) Shriver, D. F.; Drezdon, M. A. *The Manipulation of Air-Sensitive Compounds*, 2nd ed.; Wiley: New York, 1986.
(26) Kienzle, A. PhD Thesis, University of Stuttgart, Stuttgart, Germany, 1994.

Table 1. Methanolysis of Monomer TDB, Tris(1-(dichloro(methyl)silyl)ethyl)borane, and Subsequent Hydrolysis of the Reaction Product with Different Amount of Water for the Synthesis of the Preceramic Polymers P1−P3

reaction	organosilylborane **TDB**	methanol	water	product
1	5 mL (0.0145 mol)	3.6 mL (0.089 mol)	0.6 mL (0.032 mol)	**P1**
2	5 mL (0.0145 mol)	3.6 mL (0.089 mol)	0.8 mL (0.044 mol)	**P2**
3	5 mL (0.0145 mol)	3.6 mL (0.089 mol)	1.2 mL (0.066 mol)	**P3**

An amount of 5 mL of the monomer **TDB** was then put in a 250 mL flask, solved in 50 mL of tetrahydrofuran (THF), and cooled at 0 °C. After stirring for 10 min, 3.6 mL (0.089 mol) of methanol was added dropwise and stirred at room temperature for 30 h (reaction eq 2). To obtain the polymers **P1**, **P2**, and **P3**, a defined amount of water dissolved in 10 mL of THF was added after methanolysis, to promote polycondensation. The stoichiometric amounts of water used for the hydrolysis step are summarized in Table 1. All samples were subsequently cross-linked at 150 °C for 10 h under vacuum at 1×10^{-2} Torr prior to the rheological measurements.

2.2. Pyrolysis and Spectroscopic Analysis of the Preceramic Polymers. Pyrolysis experiments of the polymers were carried out in alumina crucibles in a GERO tube furnace equipped with an alumina tube under continuous argon flow. The samples were heated to 1400 °C with 150 °C h^{-1}. Heating was then automatically turned off and the samples were cooled to room temperature.

2.2.1. NMR and IR Spectroscopy. The polymers were characterized using NMR and Fourier transform infrared (FT-IR) spectroscopy. NMR spectra were recorded on a Bruker DRX 500 spectrometer (99.4 MHz for ^{29}Si and 160.5 MHz for ^{11}B) using C_6D_6 as solvent. Shifts are given relative to external tetramethylsilane (^{29}Si) and borontrifluoride diethyletherate (^{11}B). FT-IR spectra were recorded on a Perkin-Elmer FT-IR 1750 using a diamond single reflection ATR unit from Specac Inc. (U.K.).

2.2.2. Mass Spectrometry. Mass spectra were recorded by means of a Kratos MS 50 spectrometer at the Institute of Inorganic Chemistry at the University of Bonn, Germany. MALDI (Matrix Assisted Laser Desorption/Iozation) was used as ionizing method with DCTB (3-methyl-4-(4-tert-butylphenyl)butadiene-1,1-dinitrile) as matrix. In the case of compounds containing isotopes, the *m/z* data are related to the sum of the combination of the respected isotopes with the highest relative frequency. The detected ions are given in mass per charge (*m/z*) values, the relative intensities are given in percentage and the resulting stoichiometric formula. The analyzed atomic composition is based on the expected isotopic pattern.

2.2.3. Thermal and Elemental Analysis. Thermal analysis was performed with a simultaneous thermal analyzer STA 429 (Netzsch, Germany). The gases evolved during pyrolysis were detected in situ with a Balzers QMA 400 mass spectrometer coupled to the STA equipment. Thermal gravimetric analysis (TGA) experiments were conducted at a heating rate of 5 °C min^{-1} under argon flow. The Si, B, and Cl contents of the ceramics were analyzed by Mikrolabor Pascher, Remagen, Germany. The C and O content of the ceramics were measured by hot gas extraction using a NO-Analyzer Leco TC-436 and a C-Analyzer Leco C-200, respectively.

2.2.4. Microstructural and Nanochemical Analyses of the Ceramic Products. The local phase composition and the microstructural features of the fragmented SiBCO ceramics after thermal treatment at 1400 °C were investigated by high resolution transmission electron microscopy (HRTEM), scanning electron microscopy (SEM), and electron energy-loss spectroscopy (EELS), especially of the near-edge fine structures (ELNES). The finely dispersed powder of the sample under study was placed on a carbon-coated copper grid. The HREM and EELS investigations were carried out in a combined scanning/transmission electron microscope (TEM/STEM, CM 20 FEG, Philips, Eindhoven, The Netherlands) having a point resolution of 0.24 nm and an operating voltage of 200 kV, equipped with a postcolumn electron energy filter (Gatan Imaging Filter GIF 200, model 667, Pleasanton, CA) as well as with a digital scanning module (Gatan Digiscan). EELS was performed with an energy resolution of about 0.8 eV. Point analyses were made in the nanoprobe mode with the electron probe of a few nanometers in diameter. For spectrum processing the software packages Digital Micrograph and EL/P of Gatan were used.

2.2.5. Rheological Measurements. The rheological measurements were performed under a nitrogen atmosphere using a Physica UDS200 rotational rheometer, which was integrated in a glovebox. The geometry selected for these experiments was a plate-plate geometry (nominal gap, 1 mm; diameter, 25 mm), and 0.5 g of each sample was placed between the preheated plates. The measurements included the determination of the viscosity subject to temperature, time and shear rate as well as the characterization of the viscoelastic properties using oscillation experiments.

3. Results and Discussion

3.1. Synthesis of Boron-Containing Polysiloxanes. According to eq 1, methanolysis of tris(1-(dichloro(methyl)silyl)ethyl)borane (**TDB**) results in the formation of tris(1-(dimethoxy(methyl)silyl)ethyl)borane. ^{11}B-NMR-studies of the reaction product exhibit two chemical shift values at $\delta = 82.9$ and 53.5 ppm indicating the presence of trigonally planar coordinated boron.[27,29] The shift value at 82.9 ppm is assigned to boron 3-fold coordinated by carbon atoms whereas the chemical shift value at 53.5 ppm is explained by the presence of boric acid esters of the type $R_2B(O\text{-}CH_3)$ formed by partial reaction of CH_3OH with B−C bonds during methanolysis.[28] Thus, the reaction of methanol with **TDB** in part results in the cleavage one B−C bond. The cleavage of further B−C bonds during methanolysis of **TDB** can be excluded because other boric acid esters such as $RB(O\text{-}CH_3)_2$ should give rise to additional chemical shift values in the range of 30−40 ppm.

Moreover, ^{29}Si NMR analysis revealed the presence of two groups of chemical shift values located in the ranges between −1 and −5 ppm and between 13 and 17 ppm. The low-field chemical shift values are related to the presence of residual chlorine atoms bonded to silicon, whereas the high-field shifts values between −1 and −5 ppm are due to the formation of methoxysilane groups as published by van den Berghe.[29]

Mass spectrometric studies of the methanolyzed TDB clearly showed that the reaction did not result in the complete substitution of the chlorine atoms. This finding is confirmed by the analyzed fragment units found in the mass spectrum

(27) Brown, H. C. Process for Producing Dimethylorganoboranes U.S. Patent 5276195, 1994.
(28) Brown, H. C.; Vasumathi, N. *Organometallics* **1993**, *12*, 1058–1067.
(29) Van den Berghe, E. V.; Van der Kelen, G. P. *J. Organomet. Chem.* **1976**, *122*, 329–334.

4

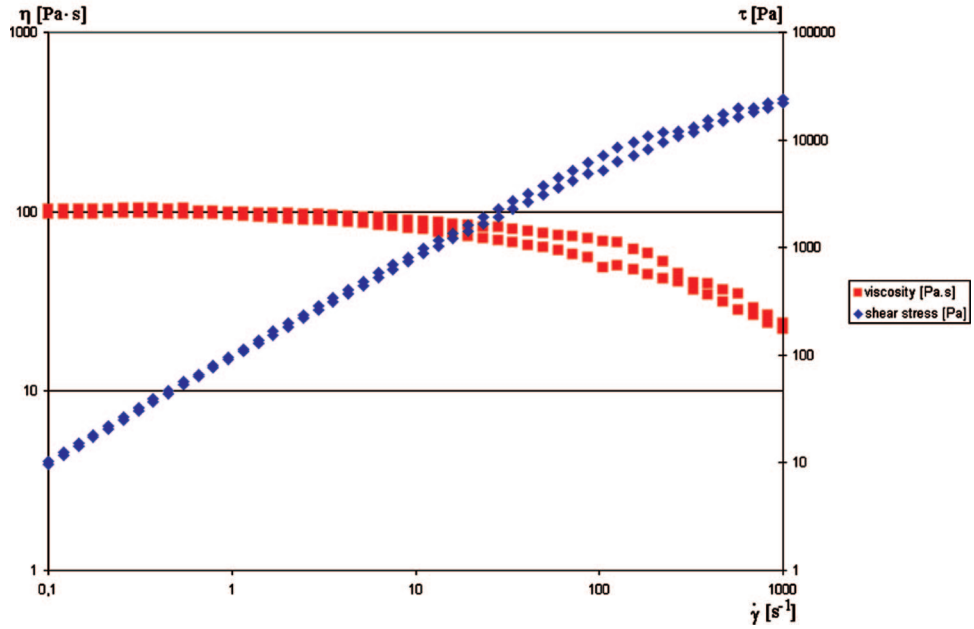

Figure 1. Flow characteristics of polymer **P2** at 93 °C.

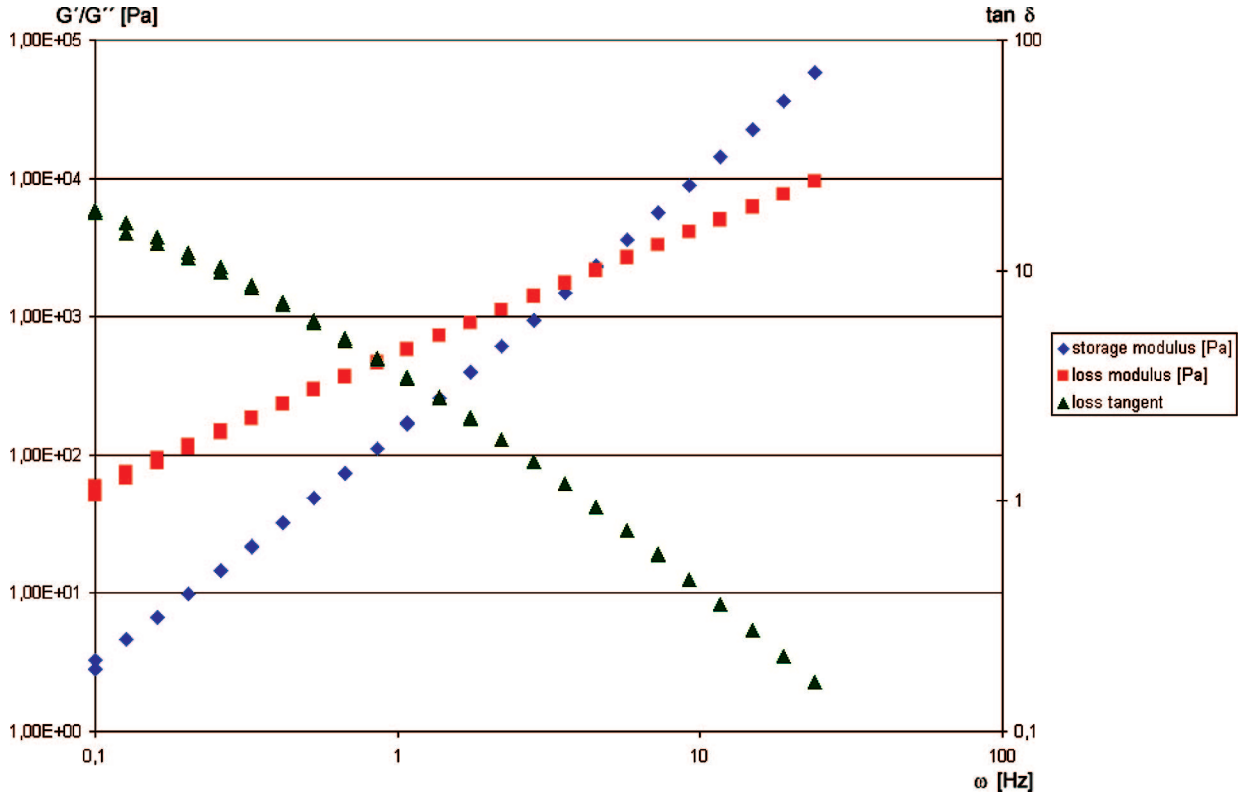

Figure 2. Dependence of the dynamic moduli (storage modulus G' and loss modulus G'', respectively) and the loss tangent from the oscillation frequency at 93 °C and a deformation of 0.1 for polymer **P2**.

with *m*/*z* 285.0 and 281.1. The isotopic ratio of the two mass peaks can be assigned to the following fragment units: $[B(CH(CH_3)SiCH_3(OCH_3)Cl)_2]^+$ (285.0) and $[(CH_3O)_2$-$CH_3SiCH(CH_3)BCH(CH_3)SiCH_3(OCH_3)Cl]^+$ (281.1).

In addition, a fragment unit corresponding to the fully methanolyzed product was also found at *m*/*z* 277.1 and assigned to $[B(CH(CH_3)SiCH_3(OCH_3)_2)_2]^+$.

After hydrolysis of the methanolyzed monomer **TDB** with different amounts of H_2O according to eq 3, the obtained polymers were investigated by IR and NMR, prior to rheological measurements. FT-IR studies showed absorption bands assigned to the presence of asymmetric stretching B−C vibration at 1100 cm^{-1} and symmetric deformation vibration of Si-CH_3 bonds at 1250 cm^{-1} in the hydrolyzed samples. Absorption bands

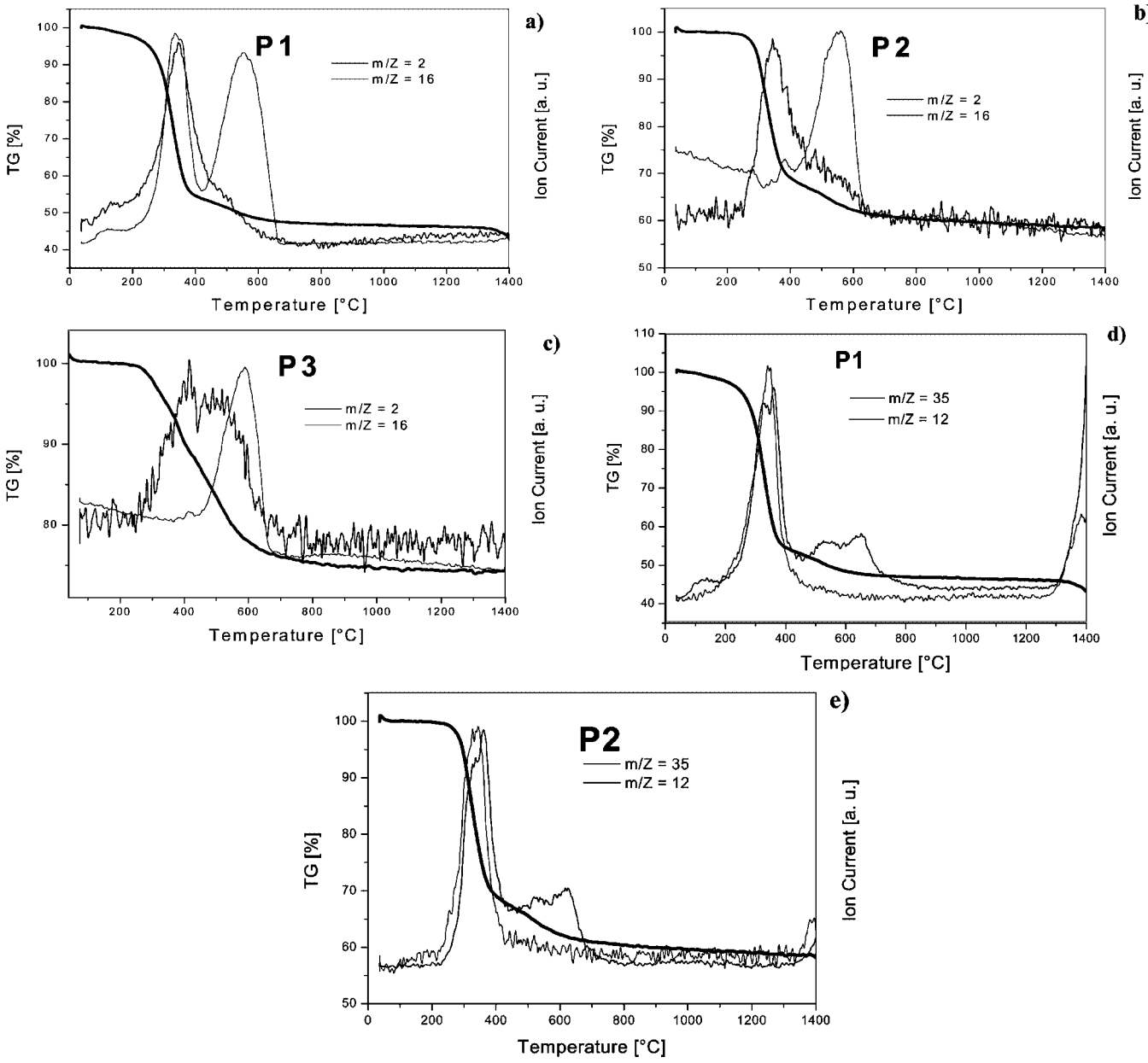

Figure 3. Thermal gravimetric analysis with in situ mass spectroscopy measurements between room temperature and 1400 °C. The evolution of methane (*m*/*z* 16) and hydrogen (*m*/*z* 2) was observed for all samples (a−c). In addition, signals with *m*/*z* 12 and 35 are shown in (d) and (e). The mass *m*/*z* 12 is due to carbon fragments, whereas *m*/*z* 35 has to be assigned to chlorine and was detected for **P1** and **P2** (d, e).

Table 2. Elemental Analysis of the Ceramics C1, C2, C3 Obtained after Pyrolysis of P1, P2, and P3 at 1400 °C in Ar

	element content of the ceramics (wt %)						
	Si	B	C	O	Cl	stoichiometry of the ceramics	product
P1	38.20	4.02	28.89	28.05	<0.5	$SiB_{0.27}C_{1.77}O_{1.29}(Cl_{<0.1})$	**C1**
P2	40.20	3.79	31.83	24.10	<0.5	$SiB_{0.24}C_{1.84}O_{1.04}(Cl_{<0.1})$	**C2**
P3	37.30	4.53	26.27	30.07	<0.5	$SiB_{0.31}C_{1.65}O_{1.41}(Cl_{<0.1})$	**C3**

measured between 1000 and 1100 cm^{-1} are due to the asymmetric stretching vibration of Si−O−C (residual Si−O−Me units) and/or Si−O−Si groups, respectively.[30,31] Two broad NMR signals located at −15 and −19 ppm were revealed by ^{29}Si NMR spectra for all the samples indicating the presence of cyclic polysiloxanes.[32,33] For samples **P1**, **P2**, and **P3**, a chemical shift value around 84 ppm was detected in the ^{11}B-NMR spectra, indicating that the trigonal planar BC_3 units remained unchanged during hydrolysis. An additional signal with much lower intensity at around 54 ppm was seen in all 3 samples and is due to methanolysis as described above. We assume that boric acid derivatives of the form $R_2B(OH)$ were formed by hydrolysis of the boric acid ester $R_2B(O\text{-}CH_3)$

(30) Corriu, R. J.-P.; Douglas, W. E. *J. Inorg. Organomet. Polym.* **1993**, *3*, 129–139.
(31) Walkiewicz-Pietrzykowska, A.; Espinos, J. P. *J. Vac. Sci. Technol.* **2006**, *A24* (4), 988–994.
(32) Babonneau, F.; Thorne, K. *Chem. Mater.* **1989**, *1*, 554–558.
(33) Horn, H. G.; Marsmann, H. C. *Makromol. Chem.* **1972**, *162*, 255.

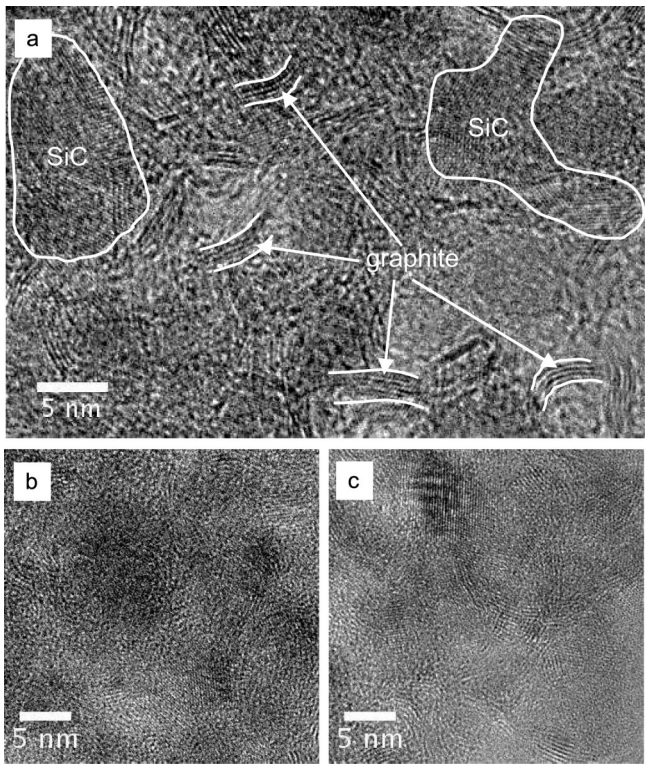

Figure 4. HREM images showing nano crystalline SiC and turbostratic graphite inclusions in the as-synthesized siBCO ceramics: (a) **C1**, (b) **C2**, and (c) **C3** samples after annealing at 1400 °C. Some SiC and graphite regions are highlighted in the higher-magnification image (a) to serve as an eye guide.

obtained as a byproduct during methanolysis of **TDB**. Such kind of boric acid species can explain the chemical shift of ~50 ppm in the ^{11}B-NMR spectra.[28]

3.2. Rheology of the Boron-Modified Polysiloxanes. Polymer **P1** was a liquid at room temperature (viscosity 7.95 Pa s at 22.4 °C). In a prolonged measurement, a slight increase of the viscosity from 7.95 to 8.25 Pa s over 30 min at 22.4 °C was found, indicating a further cross-linking even at room temperature. Polymer **P2**, a solid at room temperature, was readily meltable at elevated temperatures. The viscosity of the polymer melt was 333 Pa s at 80 °C and decreased roughly exponentially to 65.5 Pa·s at 96 °C. The determination of the flow characteristics was carried out at 93 °C (at a viscosity of 100 Pa s). The polymer melt showed pseudo plastic flow behavior (roughly Newtonian flow behavior at shear rates less than 1 s^{-1} and shear thinning at higher shear rates); see Figure 1. Deformation-dependent measurements at an oscillation frequency of 10 Hz showed that the linear visco-elastic flow behavior extends from $\gamma =$ 0 to 0.15, the loss tangent (ratio of the loss modulus G″ vs the storage modulus G′) being 0.47 in this range. Frequency-dependent measurements at an amplitude of $\gamma = 0.1$ (Figure 2) show an almost linear increase of both G' and G'' (double-logarithmic plot), the slope in the increase of G' being approximately 1.9 times as high as the slope in the increase of G''. Correspondingly, the loss tangent decreases with increasing frequency. The gel point ($G' = G''$) is found at 4 Hz.

The relatively low loss tangent at 10 Hz/$\gamma = 0.1$, as well as its slight but readily identifiable deviation from linear decrease (double-logarithmic plot) at low frequencies, indicates an already pronounced degree of cross-linking, associated with a significant elastic proportion in the flow behavior of the polymer melt. These findings indicate that the polymer should be spinnable, albeit a slightly less degree of cross-linking would be more favorable in this respect. We will report on our spinning experiments in a separate publication.

Polymer **P3** was a solid at room temperature and did not melt upon warming; thus no rheological measurements could be performed.

3.3. Thermal Decomposition of the Polysiloxanes. The thermal decomposition of the preceramic polymers during heat treatment was investigated between room temperature and 1400 °C by thermal gravimetric analysis (TGA) and by in situ mass spectroscopy (Figure 3). A main mass loss step is observed for all samples **P1**, **P2**, and **P3** between 200° and 400 °C, where most of the volatile components are released. From the DTG curves (not shown) the maximum decomposition occurs at around 300° − 380 °C for a heating rate of 5 °C/min. The samples show a nearly constant mass from 800 to 1400 °C, except for **P1**, which shows a third, slight mass loss starting at 1350 °C. The ceramic yields of the three samples are 45, 58 and 75 wt% for **P1**, **P2**, and **P3**, respectively after annealing at 1400 °C. This result reveals that the degree of cross-linking clearly influences the thermal stability and pyrolysis behavior of the preceramic polymers.

The results of the in situ mass spectroscopy measurements are shown in Figure 3. The mass loss between 200 and 700 °C is characterized by the evolution of hydrogen ($m/z = 2$) and methane ($m/z = 16$) in all three samples. Although the same species are evolved in this temperature range, the difference in the ion current curve for the signal $m/z = 16$ should be mentioned. The evolution of methane occurs in two steps for **P1**, whereas one step is the characteristic for **P2** and **P3**. This finding can be explained in terms of the molecular structure of the three polymers. Because of the different stoichiometries, **P1** still contains significant amounts of methoxy groups attached to silicon. In contrast, only residual amounts of CH_3O groups are present in **P2** and **P3**. In the case of sample **P1**, the TG curve reveals a further onset of mass loss at about 1350 °C. In this temperature range, a strong carbon signal with m/z 12 is found. The origin of the m/z 12 signal at this high temperature is still unclear. A carbothermal reaction can be excluded as the explanation for this finding, since neither SiO nor CO signals were identified in the in situ mass spectroscopic analysis. Finally, residual chlorine with m/z 35 is detected as outgassing species between 200 and 400 °C as well as between 1300 and 1400 °C in samples **P1** and **P2**. The evolution of chlorine containing species in the low temperature region proves that the methanolysis of tris(1-(dichloro(methyl)silyl)ethyl)borane **TDB** was not complete in the case of **P1** and **P2** and is in accordance with the mass spectrometric results reported above. Moreover, even hydrolysis of the methanolized monomer **TDB** did not result in the formation of Cl-free polymers. In contrast, no chlorine was found by in situ mass spectrometric analysis of polymer **P3** in the whole temperature range of our study. This finding implies that applying a high amount of water in the hydrolysis step results in chlorine-free polymers.

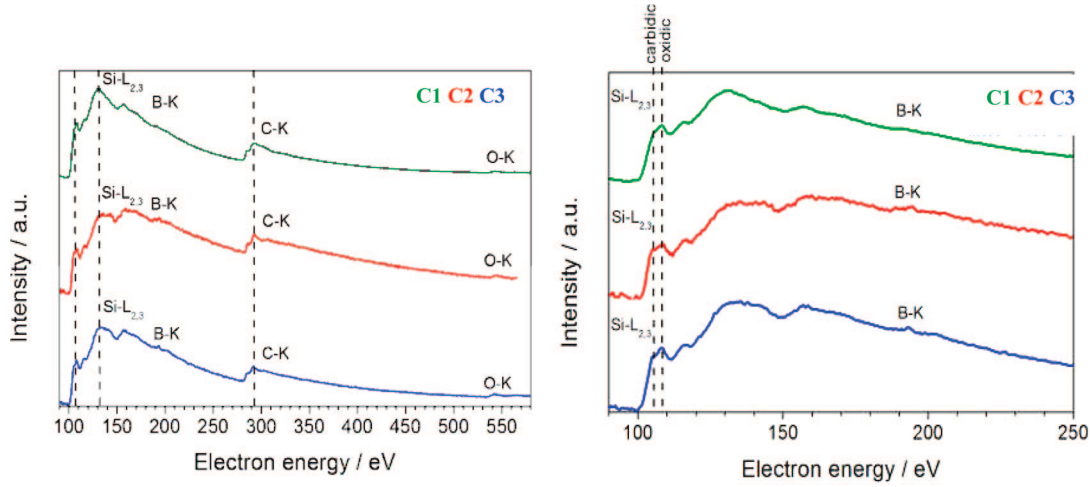

Figure 5. EELS spectra of the SiBCO ceramics **C1**, **C2**, and **C3** after annealing at 1400 °C. Right: expanded region around the Si-L_{23} ionization edge.

The elemental analyses for the polymers pyrolyzed at 1400 °C are listed in Table 2. The three samples differ in the amount of added water used for hydrolysis and cross-linking. From Table 2 it is obvious that the different amounts of water only gradually change the chemical composition of the final ceramics **C1**, **C2**, and **C3**. This gradual change can be explained by the individual decomposition behaviors of the preceramic polymers **P1**, **P2**, and **P3**. It can be also taken from Table 2 that despite the double molar amount of water reacted with **TDB** to produce polymer **P3**, the oxygen content of the resulting final SiBCO ceramic increased only by 2 wt % as compared to sample **P1**. Thus, the **TDB**/H_2O ratio during hydrolysis is rather insensitive and does not change significantly the final ceramic composition. The amount of chlorine remaining in the ceramics after pyrolysis is less than 0.5 wt % for all three materials, indicating that the residual chlorine groups in the starting precursors were removed during the heat treatment, as shown in Figure 3.

3.4. Microstructure and Nanochemistry. *3.4.1. HREM Investigations.* Nanocrystals of SiC as well as graphitic regions were observed in all the samples **C1**, **C2**, and **C3**, as demonstrated in Figure 4a−c by the arrangement and the spacings of the atomic planes. Some SiC and graphite regions are additionally marked in the higher magnified image (a) to serve as a guide to the eye. There is no distinct difference in the morphology and phase distribution: All these samples comprise an amorphous SiBCO matrix with significant inclusions of nanocrystalline SiC and more or less turbostratic graphite.

3.4.2. EELS Investigations. All the samples show both carbidic and oxidic bonding in the nearest coordination sphere of silicon. The fine structure of the C−K edge is consistent with the presence of turbostratic graphite, observed by HREM. No difference among the samples is detected by EELS, as shown in Figure 5. The degree of component segregation varies slightly within the same sample, related to the appearance of the SiC and graphite nanoinclusions in the amorphous Si−B−C−O matrix. It is clear that the sample regions with such nanoinclusions are slightly depleted of oxygen, compared to purely amorphous regions. This was also confirmed by the locally resolved EELS analyses. On the whole, the compositional variations in the sample volume are, however, insignificant at the submicrometer scale, because of the relatively small size and uniform distribution of the SiC and graphite nanoinclusions. The presence of boron in all three ceramic samples was confirmed by the appearance of the B−K edge in the EEL spectra. The quantitative and even qualitative analysis of these boron ELNES features is, however, not possible, because of overlapping of the B−K edge with ELNES features of the Si-$L_{2,3}$ edge.

4. Conclusions and Outlook

In the present work, we studied the rheological and thermal behavior of novel organoborosiloxanes as precursor for the formation of high-temperature-resistant SiBCO ceramic fibers. The preceramic polymers were synthesized via a two step reaction sequence: (i) methanolysis of tris-(1-(dichloro-(methyl)silyl)ethyl)borane (**TDB**) and (ii) hydrolysis of the reaction product with different amount of water. With this procedure, we were able to tune the rheology of the resulting polymer by adjusting the degree of cross-linking. The degree of cross-linking is a function of the amount of water used during hydrolysis. According to reaction eq 2, one mole of methanolized **TDB** contains 6 mol of hydrolyzable methoxy groups. Using 2 mol of water per mole of methanolized **TDB** for the hydrolysis step results in a low viscous polymer, whereas 4.5 mol of water provides a polymer with high melting range and high viscosity. A preceramic polymer (**P2**) with a rheological behavior optimized for fiber spinning was obtained by hydrolysis of one mole of methanolized **TDB** with 3 mol of water. In this particular sample, the melting range and the fluid mechanical behavior expressed by the dynamic moduli G' and G'' meet all the requirements for fiber spinning.

The degree of cross-linking affects the thermal decomposition of the polymers. After pyrolysis at 1400 °C in argon the ceramic yield clearly increases with the degree of cross-linking. The thermal decomposition starts at around 300 °C with the evolution of methane, hydrogen, and residual chlorine containing species. Above 800 °C the mass remains

nearly constant up to the final temperature of 1400 °C and X-ray amorphous SiBCO ceramics are obtained as reaction product. HREM reveals inclusions of turbostratic graphite and nanocristalline SiC in the amorphous SiBCO matrix. The segregation degree of components in the ceramics after annealing at 1400 °C, namely, turbostratic graphite and silicon carbide, varies only slightly with the amount of water used for the hydrolysis reaction.

The experimental results obtained in our work provide important data required for fiber spinning of preceramic polymers and for the development of high temperature resistant ceramic fibers.

Acknowledgment. The authors thank the German Research Foundation (DFG) for financial support under Grants WO 482/11-2, RI 510/36-2, and CL 208/2-2. We also thank Dr. Marianne Ensinger and Dr. Emanuel Ionescu for the measurement and discussion of the mass spectra.

CM703137E